

Parallel compression algorithm for fast preparation of defect-free atom arrays

Shangguo Zhu, Yun Long, Mingbo Pu, and Xiangang Luo*

*State Key Laboratory of Optical Technologies on Nano-Fabrication and Micro-Engineering,
Institute of Optics and Electronics, Chinese Academy of Sciences, Chengdu 610209, China
School of Optoelectronics, University of Chinese Academy of Sciences, Beijing 100049, China and
Research Center on Vector Optical Fields, Institute of Optics and Electronics,
Chinese Academy of Sciences, Chengdu 610209, China*

(Dated: December 7, 2022)

Defect-free atom arrays have emerged as a powerful platform for quantum simulation and computation with high programmability and promising scalability. Defect-free arrays can be prepared by rearranging atoms from an initial partially loaded array to the target sites. However, it is challenging to achieve large-size defect-free arrays due to atom loss during atom rearrangement and the vacuum-limited lifetime which is inversely proportional to the array size. It is crucial to rearrange atoms in fast algorithms with minimized time cost and atom loss. Here we propose a novel parallel compression algorithm which utilizes multiple mobile tweezers to transfer the atoms in parallel. The total time cost of atom rearrangement could be reduced to scale linearly with the number of target sites. The algorithm can be readily implemented in current experimental setups.

I. INTRODUCTION

Arrays of individual neutral atoms trapped in optical tweezers have emerged as a prominent and versatile platform with high programmability and promising scalability for quantum science and technology. The platform provides unique advantages, such as precise single-site control and readout, flexible geometric configuration, and low entropy, which lead to many recent breakthroughs, including quantum simulations of exotic quantum matters [1–5], high-fidelity entanglement and quantum logic operations in quantum computations [6–10], and enhanced coherence, control and readout in quantum metrology [11–13].

Compared to the approach of using optical lattices, atom arrays are built in a bottom-up way from individual atoms trapped in optical tweezers. A crucial step is the preparation of full defect-free atom array by atom rearrangement starting from an initial partially stochastically loaded atom array. Atom arrangement could be performed by dynamically changing the trap pattern generated by a spatial light modulator (SLM) [14, 15]. However, limited by the speed of SLMs, this method is only applied to small-size atom arrays. Another strategy is to use acousto-optic deflectors (AODs) which generate extra mobile tweezers to rearrange atoms in the static tweezers produced by an SLM [16–18]. The atoms can be captured from or released to the static tweezers by ramping up or down the trap depths of the mobile tweezers. The position of mobile tweezers can be dynamically controlled by changing the tone frequencies of AODs. Then the atoms are transferred to the target sites via collision-free paths, which avoid atom loss due to collisions with other atoms. Using this mobile tweezer strategy, it is promising to realize large-size defect-free atom arrays.

Due to collisions with the residual gas, the typical vacuum-limited lifetime of a single atom trapped in an optical tweezer is about 20 s [19]. The vacuum-limited lifetime of an atom array is inversely proportional to the number of atoms. Especially for large array sizes, the atom rearrangement time should be less than the lifetime of the array. In the optimal case, the atom rearrangement time should only take a small portion of the vacuum-limited lifetime so that there will be sufficient time for subsequent operations of quantum simulation or computations.

On one hand, to achieve large-size defect-free atom arrays, one can increase the vacuum-limited lifetime by improving the experimental setups and techniques. Recently, the single-atom lifetime of over 6000 s was reported for a system placed in a cryogenic environment [20], and later a defect-free array of over 300 atoms was achieved [21]. On the other hand, one can minimize the atom rearrangement time by using optimized atom rearrangement algorithms. If we only consider transferring one atom at one time by a single mobile tweezer, several algorithms were proposed, including the heuristic shortest-moves-first algorithm [16, 19], Hungarian matching algorithm [22], the compression algorithm [19], the LSAP algorithm [19], the heuristic cluster algorithm [23], and the heuristic heteronuclear algorithm for mixed-species atom arrays [24, 25]. For these single-tweezer algorithms, the number of moves is at least the number of vacancies in the target sites. This limits the number of moves to scale linearly with the number of target sites N at best. Recently, a pioneering method of simultaneously using multiple tweezers was demonstrated [3]. Later, two more multiple-tweezer algorithms were proposed [26, 27].

In this work, we propose a heuristic parallel compression algorithm (PCA), which utilizes multiple mobile tweezers to transfer atoms to the target sites in parallel. It significantly reduces the total number of effective moves, and the total travel distance of atoms during

* lxg@ioe.ac.cn

the preparation of defect-free atom arrays. As a result, the total atom rearrangement time could be reduced to scale at best linearly with the number of target sites N , and consequentially the success probability of achieving defect-free atom arrays increases. The algorithm is easy to implement and has a small computation time. It could be readily tested in current experimental setups.

II. DESCRIPTION OF THE PROBLEM

Initially the laser-cooled atoms are stochastically loaded in the optical tweezer array with a filling fraction p . After the atoms are ejected in pairs, we obtain a stochastic sub-Poissonian loading [28]. Each trap has probability p to be filled with a single atom and $1 - p$ with zero atoms. Typically, $p \approx 50\%$ [28]. By using gray-molasses loading [7, 29–33], p can be improved to be over 90%. Here and in the following discussions, we take $p = 50\%$ for simplicity. The goal is to form a full defect-free single atom array on the N target traps by rearranging the atoms through a deterministic sequence of operations.

As the vacuum-limited lifetime of an atom array scales as $1/N$, we seek an atom rearrangement algorithm with a minimized time cost. This is even more important for large-scale quantum simulators or computers when N increases. The minimized time cost of atom rearrangement shall allow sufficient time for subsequent operations of quantum simulation or computations. Moreover, reducing the total rearrangement time will increase the success probability due to fewer background gas collisions.

Using the mobile tweezers, atoms are captured from the source traps, transferred at a constant speed and released to the target traps. During the capturing or releasing process, the trap depth of the mobile tweezers are ramped up or down in a time period t_1 . Typically t_1 is about $15 \mu\text{s}$ to $60 \mu\text{s}$ [3, 26]. Let $t_2 = l/v$ be the time cost of moving an atom between two adjacent traps, where v is the speed of the mobile tweezer and l the distance between the adjacent static tweezers. Typical, the speed v is about $75 \mu\text{m/ms}$ to $130 \mu\text{m/ms}$ [3, 26]. Then, for $l = 2 \mu\text{m}$, t_2 is about $15 \mu\text{s}$ to $27 \mu\text{s}$. Overall, we can express the total rearrangement time T as

$$T = (C + R)t_1 + Dt_2. \quad (1)$$

Here C and R are the number of capturing and releasing processes, respectively. D is the total travel distance of all atoms in unit of l . To minimize the total rearrangement time, we need to minimize C , R and D . Due to the imperfect transfer of atoms between the mobile and static tweezers, each move of the atoms has a success probability less than unity. Reducing C and R would also increase the overall success probability.

To avoid atom loss due to collisions or disturbances of the trapping potential, the paths of mobile tweezers should not encounter or be too close to the filled traps.

Then, it requires relatively large spacing between the adjacent traps if we transfer an atom via a path between the adjacent rows of traps. Therefore, we only consider the collision-free paths which consist of lines connecting two adjacent traps and do not encounter any filled traps.

The atom rearrangement algorithms about how the atoms from the source traps are moved to the target traps are crucial to minimizing the total time cost and maximizing the success probability of achieving a defect-free atom array. However, an exhaustive searching for the optimal rearrangement paths are a difficult computational problem, especially for large atom array sizes. We consider the heuristic algorithms whose computation time is acceptable.

To summarize, for a superior heuristic rearrangement algorithm, we need to minimize 1) the number of captures and releases $C + R$, 2) the total travel distance D , and 3) the algorithm computation time.

III. PARALLEL COMPRESSION ALGORITHM

To maximize the efficiency of atom rearrangement under experimentally feasible conditions, we propose the heuristic PCA, in which multiple mobile tweezers are simultaneously generated to move atoms in parallel. The PCA comprises two stage: 1) parallel compression, and 2) postprocess.

In Fig. 1(a), we shows a demonstration of the parallel compression stage for a 6×6 target array. First, we identify the whole two-dimensional (2D) array as different layers, labeled as $0, 1, 2, 3, \dots$ from inside to outside. For a square lattice, each layer is a square. Starting from Layer 1, each layer is treated as a source layer, which provides movable atoms for the inner target region. The movable atoms are those which can be transferred in straight paths to the target traps in the inner target region.

We transfer the movable atoms in parallel by using a 2D AOD, which consists a set of two AODs along two different dimensions. Based on the number of movable atoms on each side of the layer, a one-dimensional (1D) array of the same number of mobile tweezers is generated by setting multiple tone frequencies of one AOD. Then, the 1D array of multiple mobile tweezers can be transferred in parallel paths along the direction perpendicular to the array by changing the tone frequency of the other AOD. The movable atoms are captured by ramping up the the trapping potential at the same time, then transferred in parallel straight paths, and released by ramping down the the trapping potential when reaching their target traps. The array of multiple mobile tweezers resembles a shuttle bus which picks up a number of passengers and drops them off at different bus stops.

In one transfer process, the number of capture processes equals to 1 and the number of release processes equals to the number of different path lengths. It would be more time-efficient if more paths have the same length.

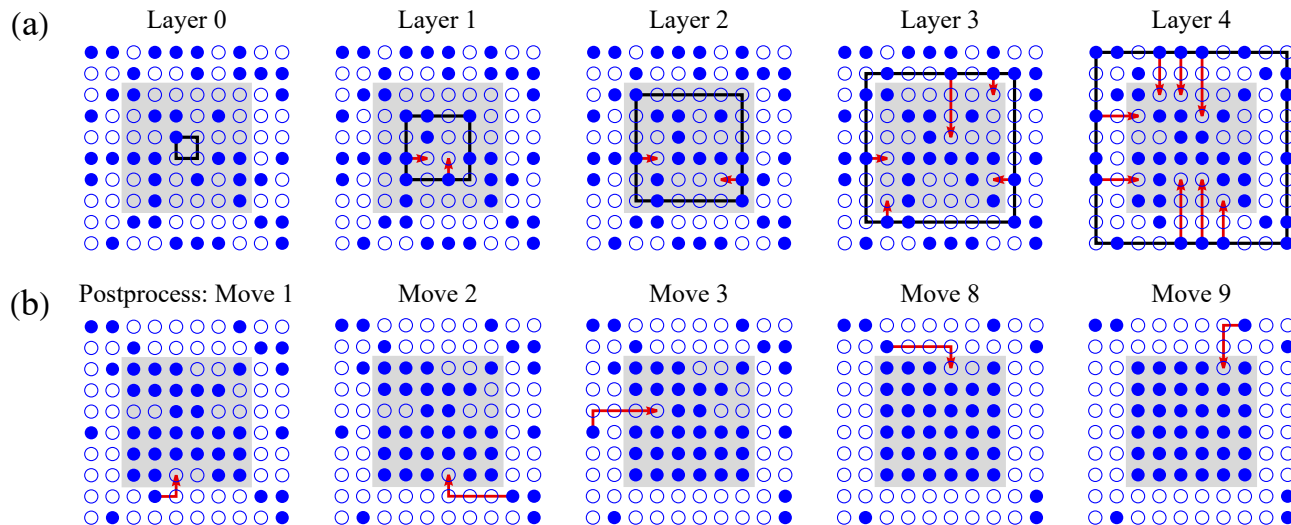


FIG. 1. Demonstration of the parallel compression algorithm (PCA) for a 6×6 target array (gray shaded region). (a) The parallel compression stage. The whole array is identified as several source layers (indicated by the black squares). Starting from Layer 1, the movable atoms on each side are transferred to the target traps in parallel with paths indicated by the red arrows. The blue dots and circles represent filled and empty traps, respectively. (b) The postprocess stage. The remaining empty traps are filled by moving the nearest available atoms. The moving paths are indicated by the red arrows with one turn.

The travel distance equals to the maximum of the path lengths.

Here we only consider using one 2D AOD to deal with one side of the layer at a time in a counterclockwise order. With more 2D AODs available, the algorithm allows a straightforward extension to an enhanced degree of parallelism by dealing with the four sides of the layer simultaneously, and this leads to a straightforward acceleration.

After the parallel compression stage, there are still a small number of empty traps in the target array. We need to perform a postprocess, demonstrated in Fig. 1(b). In the postprocess stage, the remaining empty traps are filled by moving the nearest available atoms outside the target array. The moving paths are not straight lines anymore, and in most cases consist of two successive straight paths (with one turn). The atoms are moved one at a time by one mobile tweezer without parallelism.

The idea is to transfer as many atoms as possible in the first parallel compression stage and therefore reach maximum efficiency brought by parallelism. In Sect. IV, we will show that the contribution of the postprocess stage decreases exponentially fast when we increase the number of reservoir atoms which are defined as the atoms on the initial lattice.

In the parallel compression stage, we may also flexibly choose alternative protocols according to the experimental setups. In one alternative protocol, the algorithm can be adapted to have partial parallelism. The parallel multiple mobile tweezers are generated only when the length of the paths of movable atoms are the same. In each transfer process, the atoms are captured and released in the same time sequence. The average number of parallel mobile tweezers decreases. In another alternative proto-

col, the algorithm can be adapted to have no parallelism and reduces to a single-tweezer algorithm. In the parallel compression stage, all the atoms are transferred one by one by a single mobile tweezer. Apparently, these alternative protocols result in more atom rearrangement time than the PCA with full parallelism.

IV. PERFORMANCE OF THE ALGORITHM

Here we analyze the performance of the PCA. As showed in Eq. (1), the time cost of atom rearrangement is determined by the number of capturing processes C , the number of releasing processes R , and the total distances D . To compare with other algorithms, we define the number of effective moves M as the average of the number of capturing and releasing processes,

$$M \equiv (C + R)/2. \quad (2)$$

Starting from initial stochastically loaded arrays with filling fraction $p = 50\%$, we perform simulations of the PCA and study its performance for different target array sizes. For an $L \times L$ target array (the number of target sites $N = L^2$), we start with a larger $L' \times L'$ with $L' = \lceil p^{-1/2}L + 1 \rceil$ to guarantee sufficient number of reservoir atoms for most cases. Here $\lceil x \rceil$ is the ceiling function which gives the smallest integer greater than or equal to x .

In Fig. 2, we plot M and D as functions of the number of target sites N in comparison with other contemporary atom rearrangement algorithms. We see that compared to the heuristic cluster algorithm (HCA) [23], the A* searching algorithm (ASA) [23], and the heuristic path-

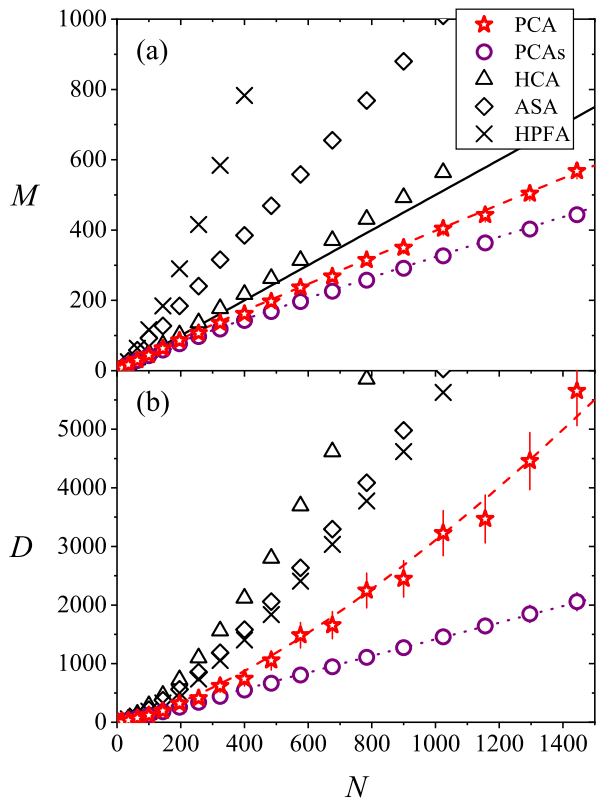


FIG. 2. The number of effective moves M in (a) and the total travel distance D in (b) as functions of the number of target sites N for different atom rearrangement algorithms, PCA (red stars), PCAs (purple circles), HCA (black triangles), ASA (black diamonds) and HPFA (black crosses). PCAs represents PCA with saturated reservoir atoms when the reservoir-to-target ratio $r \gtrsim 3$. The red dashed and purple dotted curves represent the corresponding fitting with functions showed in Eqs. (5) and (7), respectively. In (a), the black solid line represents $N/2$. The PCA and PCAs data points are averaged over 10000 simulations and the error bars show the standard deviations. The HCA, ASA, and HPFA data points are taken from Ref. [23].

finding algorithm (HPFA) [16, 23], the PCA has a significant improvement on performance in both M and D . In Fig. 2(a), the PCA is considerably below the $N/2$ limit for initial arrays with 50% filling fraction. From fitting, we find the scaling functions in the parallel compression and post process stages, respectively,

$$C_{\text{para}} \approx 2.887N^{1/2}, \quad R_{\text{para}} \approx 0.396N, \quad D_{\text{para}} \approx 0.60N, \quad (3)$$

$$C_{\text{post}} = R_{\text{post}} \approx 0.154N, \quad D_{\text{post}} \approx 0.079N^{3/2}. \quad (4)$$

As a result, we find the number of effective moves and the total travel distance

$$M \approx 0.35N + 1.44N^{1/2}, \quad D \approx 0.079N^{3/2} + 0.60N. \quad (5)$$

The acceleration of the algorithm is due to much more efficient parallel transfers of atoms by multiple mobile

tweezers in the parallel compression stage. We see that C_{para} scales as $N^{1/2}$ because the atoms are captured by multiple mobile tweezers in parallel for a number of times roughly equal to the number of sides of all the layers. R_{para} scales as N because there might be multiple stops for releasing atoms. If the releasing process could be optimized such that the array of mobile tweezers does not stop while releasing atoms, R_{para} could be further improved to be equal to C_{para} and therefore $\propto N^{1/2}$. D_{para} scales as N because it roughly equals to C_{para} times the average distance in one parallel transfer (roughly $\propto N^{1/2}$).

In the postprocess stage, we see that C_{post} and R_{post} scale as N , and D_{post} scales as $N^{3/2}$. There is no acceleration by parallelism as the atoms are transferred to the remaining target sites one at a time. This contributes to a considerable time cost at large N due to greater scaling exponents. Fortunately, the contribution of the postprocess stage can be mitigated by increasing the size of the initial array L' . By choosing $L' = \lceil (3/p)^{1/2}L \rceil$, the contribution of the postprocess stage becomes negligible, and M and D approach their saturation values, which are showed in Fig. 2 indicated as PCAs. From fitting, we find the saturation values approximately

$$\bar{C}_{\text{para}} \approx 4.6N^{1/2}, \quad \bar{R}_{\text{para}} \approx 0.50N, \quad \bar{D}_{\text{para}} \approx 1.4N, \quad (6)$$

and therefore

$$\bar{M} \approx 0.25N + 2.3N^{1/2}, \quad \bar{D} \approx 1.4N. \quad (7)$$

We see that in the saturation case, the number of effective moves and the total travel distance are determined by the parallel compression stage. The total travel distance scales as N . For an optimized releasing process in which the mobile tweezers do not stop while releasing atoms, the number of effective moves can be further improved to scale as $N^{1/2}$ and the algorithm reaches its maximum efficiency.

We also check how fast M and D approach their saturation values when increasing the size of the initial array L' . We perform simulations with the same L and multiple values of L' . Here we choose $\lceil p^{-1/2}L + 1 \rceil \leq L' \leq \lceil (3/p)^{1/2}L \rceil$. In Fig. 3, we plot the number of moves M_{post} and the total travel distance D_{post} in the postprocess stage as functions of the reservoir-to-target ratio $r \equiv pL'^2/L^2$, defined as the ratio between the average number of reservoir atoms and the number of target sites. We see that both M_{post} and D_{post} decrease as exponentially decaying functions of r when r increases. The rate of decreasing is faster for larger target arrays (with greater N). Thus, if we increase the reservoir atoms by an appropriate amount, the contribution from the postprocess stage decays exponentially fast. Then a vast majority of atom transfers are completed in the parallel compression stage. In this way, we could enjoy the acceleration brought by parallelism to full extent.

The PCA is very easy to be implemented in a regular computer program. It takes relatively small computation

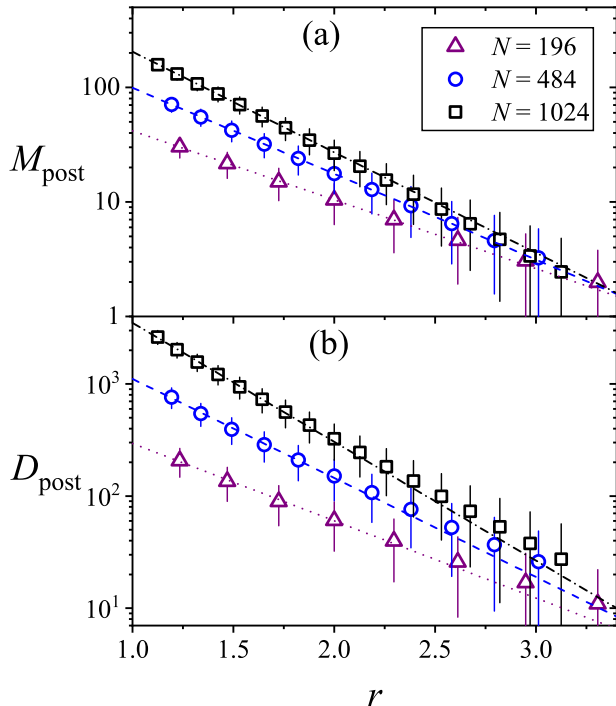


FIG. 3. The number of moves M_{post} in (a) and the total travel distance D_{post} in (b) in the postprocess stage as functions of the reservoir-to-target ratio r , for the numbers of target sites $N = 196$ (purple triangles), $N = 484$ (blue circles), and $N = 1024$ (black squares). The purple dotted, blue dashed and black dash-dotted lines respectively represent the corresponding fitting with exponentially decaying functions $M_{\text{post}} \approx 166.1e^{-1.384r}$, $556.9e^{-1.727r}$, $1544e^{-2.020r}$ in (a), and $D_{\text{post}} \approx 1439.1e^{-1.587r}$, $8478.3e^{-2.034r}$, $40205e^{-2.441r}$ in (b). The points are averaged over 10000 simulations and the error bars show the standard deviations.

time, about 1.8 ms on average for a 14×14 target array on a regular laptop computer with 8 CPU cores (Intel Core i7-1165G7) and 16 GB of RAM.

V. SUMMARY

In summary, we have proposed an efficient atom rearrangement algorithm, the parallel compression algorithm, which provides a superior way of rearranging atoms starting from an initial partially stochastically loaded array to form a full defect-free atom array. The core idea is to divided the array into layers and to transfer multiple movable atoms in each layer by multiple mobile tweezers in parallel. The total time cost could be reduced to scale linearly as N , which is huge improvement compared to the contemporary single-tweezer algorithms. Moreover, the algorithm is easy to be implemented and have a small computation time.

The parallel compression algorithm will have important and vast applications in quantum simulation and computation in the noisy intermediate-scale quantum era. By combining the algorithm with state-of-art experimental techniques such as the gray-molasses loading for higher filling fractions [7, 29–33] and the cryogenic environment for longer vacuum-limited lifetime [20, 21], even larger size of defect-free atom arrays could be achieved in experiments in the near future.

-
- [1] A. Browaeys and T. Lahaye, Nat. Phys. **16**, 132 (2020), URL <https://www.nature.com/articles/s41567-019-0733-z>.
- [2] A. M. Kaufman and K.-K. Ni, Nat. Phys. pp. 1–10 (2021), URL <https://www.nature.com/articles/s41567-021-01357-2>.
- [3] S. Ebadi, T. T. Wang, H. Levine, A. Keesling, G. Semeghini, A. Omran, D. Bluvstein, R. Samajdar, H. Pichler, W. W. Ho, et al., Nature **595**, 227 (2021), URL <http://dx.doi.org/10.1038/s41586-021-03582-4>.
- [4] P. Scholl, M. Schuler, H. J. Williams, A. A. Eberharter, D. Barredo, K.-N. Schymik, V. Lienhard, L.-P. Henry, T. C. Lang, T. Lahaye, et al., Nature **595**, 233 (2021), URL <http://dx.doi.org/10.1038/s41586-021-03585-1>.
- [5] G. Semeghini, H. Levine, A. Keesling, S. Ebadi, T. T. Wang, D. Bluvstein, R. Verresen, H. Pichler, M. Kalinowski, R. Samajdar, et al., Science **374**, 1242 (2021), URL <http://dx.doi.org/10.1126/science.abi8794>.
- [6] H. Levine, A. Keesling, G. Semeghini, A. Omran, T. T. Wang, S. Ebadi, H. Bernien, M. Greiner, V. Vuletić, H. Pichler, et al., Phys. Rev. Lett. **123**, 170503 (2019), URL <http://dx.doi.org/10.1103/PhysRevLett.123.170503>.
- [7] A. Jenkins, J. W. Lis, A. Senoo, W. F. McGrew, and A. M. Kaufman, Phys. Rev. X **12**, 021027 (2022), URL <https://link.aps.org/doi/10.1103/PhysRevX.12.021027>.
- [8] S. Ma, A. P. Burgers, G. Liu, J. Wilson, B. Zhang, and J. D. Thompson, Phys. Rev. X **12**, 021028 (2022), URL <https://link.aps.org/doi/10.1103/PhysRevX.12.021028>.
- [9] T. M. Graham, Y. Song, J. Scott, C. Poole, L. Phuttitarn, K. Jooya, P. Eichler, X. Jiang, A. Marra, B. Grinkemeyer, et al., Nature **604**, 457 (2022), URL <http://dx.doi.org/10.1038/s41586-022-04603-6>.
- [10] D. Bluvstein, H. Levine, G. Semeghini, T. T. Wang, S. Ebadi, M. Kalinowski, A. Keesling, N. Maskara, H. Pichler, M. Greiner, et al., Nature **604**, 451 (2022), URL <http://dx.doi.org/10.1038/s41586-022-04592-6>.
- [11] I. S. Madjarov, A. Cooper, A. L. Shaw, J. P. Covey, V. Schkolnik, T. H. Yoon, J. R. Williams, and M. Endres, Phys. Rev. X **9**, 041052 (2019), URL

- <https://link.aps.org/doi/10.1103/PhysRevX.9.041052>.
- [12] M. A. Norcia, A. W. Young, W. J. Eckner, E. Oelker, J. Ye, and A. M. Kaufman, *Science* **366**, 93 (2019), URL <http://dx.doi.org/10.1126/science.aay0644>.
- [13] A. W. Young, W. J. Eckner, W. R. Milner, D. Kedar, M. A. Norcia, E. Oelker, N. Schine, J. Ye, and A. M. Kaufman, *Nature* **588**, 408 (2020), URL <http://dx.doi.org/10.1038/s41586-020-3009-y>.
- [14] H. Kim, W. Lee, H.-G. Lee, H. Jo, Y. Song, and J. Ahn, *Nat. Commun.* **7**, 13317 (2016), URL <http://dx.doi.org/10.1038/ncomms13317>.
- [15] W. Lee, H. Kim, and J. Ahn, *Opt. Express* **24**, 9816 (2016), URL <http://dx.doi.org/10.1364/OE.24.009816>.
- [16] D. Barredo, S. de Léséleuc, V. Lienhard, T. Lahaye, and A. Browaeys, *Science* **354**, 1021 (2016), URL <http://dx.doi.org/10.1126/science.aah3778>.
- [17] M. Endres, H. Bernien, A. Keesling, H. Levine, E. R. Anschuetz, A. Krajenbrink, C. Senko, V. Vuletic, M. Greiner, and M. D. Lukin, *Science* **354**, 1024 (2016), URL <http://dx.doi.org/10.1126/science.aah3752>.
- [18] D. Barredo, V. Lienhard, S. de Léséleuc, T. Lahaye, and A. Browaeys, *Nature* **561**, 79 (2018), URL <http://dx.doi.org/10.1038/s41586-018-0450-2>.
- [19] K.-N. Schymik, V. Lienhard, D. Barredo, P. Scholl, H. Williams, A. Browaeys, and T. Lahaye, *Phys. Rev. A* **102**, 063107 (2020), URL <https://link.aps.org/doi/10.1103/PhysRevA.102.063107>.
- [20] K.-N. Schymik, S. Pancaldi, F. Nogrette, D. Barredo, J. Paris, A. Browaeys, and T. Lahaye, *Phys. Rev. Applied* **16**, 034013 (2021), URL <https://link.aps.org/doi/10.1103/PhysRevApplied.16.034013>.
- [21] K.-N. Schymik, B. Ximenez, E. Bloch, D. Dreon, A. Signoles, F. Nogrette, D. Barredo, A. Browaeys, and T. Lahaye, *Phys. Rev. A* **106**, 022611 (2022), URL <https://link.aps.org/doi/10.1103/PhysRevA.106.022611>.
- [22] W. Lee, H. Kim, and J. Ahn, *Phys. Rev. A* **95**, 053424 (2017), URL <https://link.aps.org/doi/10.1103/PhysRevA.95.053424>.
- [23] C. Sheng, J. Hou, X. He, P. Xu, K. Wang, J. Zhuang, X. Li, M. Liu, J. Wang, and M. Zhan, *Phys. Rev. Research* **3**, 023008 (2021), URL <https://link.aps.org/doi/10.1103/PhysRevResearch.3.023008>.
- [24] C. Sheng, J. Hou, X. He, K. Wang, R. Guo, J. Zhuang, B. Mamat, P. Xu, M. Liu, J. Wang, et al., *Phys. Rev. Lett.* **128**, 083202 (2022), URL <https://link.aps.org/doi/10.1103/PhysRevLett.128.083202>.
- [25] K. Singh, S. Anand, A. Pocklington, J. T. Kemp, and H. Bernien, *Phys. Rev. X* **12**, 011040 (2022), URL <https://link.aps.org/doi/10.1103/PhysRevX.12.011040>.
- [26] W. Tian, W. J. Wee, A. Qu, B. J. M. Lim, P. R. Datla, V. P. W. Koh, and H. Loh (2022), arXiv:2209.08038, URL <http://arxiv.org/abs/2209.08038>.
- [27] S. Wang, W. Zhang, T. Zhang, S. Mei, Y. Wang, J. Hu, and W. Chen (2022), arXiv:2210.10364, URL <http://arxiv.org/abs/2210.10364>.
- [28] N. Schlosser, G. Reymond, I. Protsenko, and P. Grangier, *Nature* **411**, 1024 (2001), URL <http://dx.doi.org/10.1038/35082512>.
- [29] T. Grünzweig, A. Hilliard, M. McGovern, and M. F. Andersen, *Nat. Phys.* **6**, 951 (2010), URL <https://www.nature.com/articles/nphys1778>.
- [30] B. J. Lester, N. Luick, A. M. Kaufman, C. M. Reynolds, and C. A. Regal, *Phys. Rev. Lett.* **115**, 073003 (2015), URL <https://link.aps.org/doi/10.1103/PhysRevLett.115.073003>.
- [31] M. O. Brown, T. Thiele, C. Kiehl, T.-W. Hsu, and C. A. Regal, *Phys. Rev. X* **9**, 011057 (2019), URL <https://link.aps.org/doi/10.1103/PhysRevX.9.011057>.
- [32] M. M. Aliyu, L. Zhao, X. Q. Quek, K. C. Yellapragada, and H. Loh, *Phys. Rev. Research* **3**, 043059 (2021), URL <https://link.aps.org/doi/10.1103/PhysRevResearch.3.043059>.
- [33] J. Ang'ong'a, C. Huang, J. P. Covey, and B. Gadway, *Phys. Rev. Research* **4**, 013240 (2022), URL <https://link.aps.org/doi/10.1103/PhysRevResearch.4.013240>.